energies

MDPI

Article

PI Parameter Influence on Underfloor Heating Energy Consumption and Setpoint Tracking in nZEBs

Tuule Mall Kull [1,*], Martin Thalfeldt [1] and Jarek Kurnitski [1,2]

[1] Nearly Zero Energy Buildings Research Group, Tallinn University of Technology, Ehitajate tee 5, 19086 Tallinn, Estonia; martin.thalfeldt@taltech.ee (M.T.); jarek.kurnitski@taltech.ee (J.K.)
[2] Department of Civil Engineering, Rakentajanaukio 4 A, Aalto University, FI-02150 Espoo, Finland
* Correspondence: tuule.kull@taltech.ee

Received: 20 March 2020; Accepted: 17 April 2020; Published: 21 April 2020

Abstract: In rooms with underfloor heating (UFH), local on–off controllers most often regulate the air temperature with poor accuracy and energy penalties. It is known that proportional–integral (PI) controllers can regulate most processes more precisely. However, hydronic UFH systems have long time constants, especially in low-energy buildings, and PI parameters are not easy to set manually. In this work, several potential PI parameter estimation methods were applied, including optimizing the parameters in GenOpt, calculating the parameters based on simplified models, and tuning the parameters automatically in Matlab. For all found parameter combinations, the energy consumption and control precision were evaluated. Simpler methods were compared to the optimal solutions to find similar parameters. Compared with an on–off controller with a 0.5 K dead-band, the best PI parameter combination found was with a proportional gain of 18 and an integration time of 2300 s, which could decrease the energy consumption for heating by 9% and by 5% compared with default PI parameters. Moreover, while GenOpt was the best method to find the optimal parameters, it was also possible with a simple automatic test and calculation within a weekend. The test can be, for example, 6-h setbacks applied during the nights or weekend-long pseudo-random changes in the setpoint signal. The parameters can be calculated based on the simplified model from these tests using any well-known simple method. Results revealed that the UFH PI controller with the correct parameters started to work in a predictive fashion and the resulting room temperature curves were practically ideal.

Keywords: IDA ICE; building simulation; intermittent heating; model predictive control (MPC); heat pumps; proportional–integral–derivative (PID) control; thermostats

1. Introduction

The change towards nearly zero-energy buildings (nZEBs) and renewable energy sources influences the technologies used for heating and its control [1,2]. The intermittent production of renewable electricity calls for flexibility in all consumers, including buildings [3]. Space heating is responsible for up to 70% of the final energy demand in residential buildings [4]. Therefore, it has a high potential for flexibility. In modern buildings, the use of heat pumps has intensified [5]. Only electricity-based heating is relevant to the power grid, therefore, heat pumps are a clear target.

To be exploited when the grid needs it, heat pumps should use an electricity price or other signal for optimizing their performance. Some of the heat pumps already optimize their behaviour according to the price. As one solution to improve the flexibility, model predictive control (MPC) can be used [6,7]. It enables the use of historic and forecasted data to predict the most optimal course of action. At the occurrence of renewed data, the optimization can be corrected. For an MPC for a single-family house,

the input signal is, for example, the electricity price or other signal from the grid and the output of the optimization are the air temperature setpoints of the rooms [3].

The setpoints in rooms have to be tracked by room-based controllers, such as thermostats or proportional–integral–derivative (PID) controllers, as the supervisory control can deal with optimization but not with the local fast changes [8]. PID is commonly known to be one of the best and easiest feedback controllers for any process. For buildings, as a relatively slow system, the derivative part is usually dropped and PI controllers are used instead. However, choosing improper PID gains (parameters) could result in making the whole system unstable. Therefore, designers and researchers often turn to optimal or predictive solutions [9].

However, advanced solutions are not easy to implement and the need for robust and reliable solutions with minimal human interaction is evident. [10,11]. To simplify or avoid technicians' inputs to the systems, the control algorithms can be tested in realistic environments [12]. Also, building blocks have been developed to be compatible with detailed modelling so that engineers can do the tuning. However, the process is still not fully automated [13]. Auto-tuning of PID controllers for heating, cooling, and ventilation plants have been described both several decades ago [14–16] and more recently [17]. If there is enough computational power, artificial neural network models could theoretically tune their PID parameters [18].

Self-learning PI controllers are already commonly available for radiators in new buildings. As radiators are also installed in public and commercial buildings, there is a lot of interest and financial capability to develop better-performing solutions for these environments. In homes, hydronic underfloor heating (UFH) has become more popular, being a low-temperature solution that matches with heat pumps in nZEBs. For hydronic underfloor heating, even in modern buildings, only simple thermostats with a dead-band of at least 0.5 K are often used. However, using UFH with a thermostat, the air temperatures fluctuates significantly and, therefore, the users can easily raise the setpoints to avoid lower levels and to meet their comfort limits. This ends up in a higher energy consumption.

Control of underfloor heating as a slow system with a high thermal mass is a debated question, where good solutions have not been found yet. Some manufactures offer sophisticated self-learning controls, while on–off is likely the most common implementation in practice, and in some studies, self-regulating properties (no-control) have shown similar performance with more sophisticated control solutions [19]. The long time constant of UFH is even increased by a low supply temperature from heat pumps and this is due to the small losses in well-insulated nZEBs with heat recovery ventilation. This means that setting PI parameters manually by trial and error, which is the common practice for PI tuning, would take a lot of time. For self-tuning controllers, simple tests would be needed but also these can be too time-consuming.

When the gains are optimized, PID control can save energy in UFH control compared with the standard on–off control [20]. However, the optimal parameter values are usually not revealed. There is almost no previous published data on PI parameter values for UFH, with rare exceptions [21]. Furthermore, the effect of different parameters has not been analyzed for UFHs. However, the effects of PI parameters have been analyzed for radiators, as the heating circuits are, in reality, often not tuned and there is a lot of potential for energy saving [22]. Tuning radiator PID parameters with machine learning has shown a 32% reduction in heating energy consumption compared with Ziegler–Nichols tuning [23]. The current situation shows that while PID and on–off control waste energy, more advanced solutions on the market do not ensure comfort [24]. With quality tuning, PID could both reduce wasting energy and ensure comfort. The parameter optimization for UFH has been performed in extensive simulations [20], but it remains unknown whether it is possible to obtain the optimal parameters with shorter tests.

Therefore, the aim of this work is two-fold. Firstly, to determine how UFH control can be improved by the application of PI parameters specifically derived for underfloor heating in nZEB with various tests and methods. Secondly, to find whether it is possible to determine the PI parameters which perform close to optimal, when using short tests and simple methods. This work estimates the PI

parameters for UFH in nZEB and analyzes their effect on the energy performance and indoor air temperature of the building. PI performance is compared with a traditional thermostat's performance in the same situation. Both an accurate temperature tracking performance and a considerable energy saving compared with conventional control are expected. The results may be utilized in the design of UFH systems with accurate temperature control and energy savings compared with conventional UFH systems.

2. Materials and Methods

2.1. The Building

The work is based on a test building at TalTech University campus, which is described in detail in several previous publications [25–27]. Two almost identical rooms with a floor area of 10.4 m^2 were analyzed, except that one of them (Room 6 or R6) has two 4 m^2 windows facing south and west, while the windows of the other (Room 5 or R5) face north and west. The floor plan of the building is shown in Figure 1 with the two test rooms highlighted with red rectangles. Previously, the test house model in IDA ICE 4.8 software [28] was calibrated against measured air temperatures in the test room R5 during temperature setback cycles with varying durations [27]. As a result, the heat losses and thermal mass of the room structures are adequately defined in the model. This model was used for the simulations in the current work. In the simulations, all of the other rooms were heated constantly with ideal heaters to the setpoint of 21 °C.

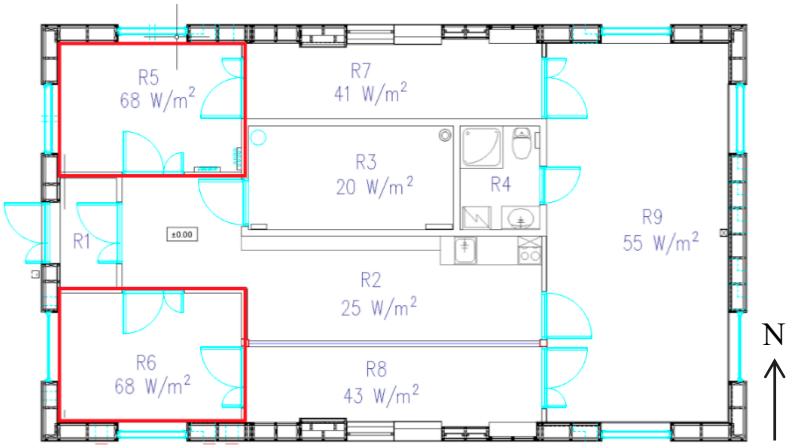

Figure 1. Layout of the test building; the two test rooms are shown in red rectangles.

The building has wooden-frame walls, a wooden-frame roof, and concrete floors with a crawl space below. The total heat-up time constant for the rooms is around 85 h and the effective time constant for temporary setbacks is around 12 h [27]. The absolute cool-down time constant of one test room is around 24 h when the other rooms are heated constantly. The time constant for the whole building cool-down is ca. 100 h. The time constants are long mainly due to the concrete floor and highly insulated building envelope. The values were confirmed by the experimental data presented in [27].

2.2. Outline of the Work

The PI parameters were estimated for the two test rooms in several different ways. Firstly, they were optimized in GenOpt with the aim of minimal setpoint tracking errors both for the constant and variable setpoints (Section 2.5). Secondly, they were calculated and estimated using simplified models. The data used for the model fitting are described in Section 2.3 and the model fitting process is described in Section 2.4. The models were used to either autotune the parameters in Matlab or to calculate the parameters using well-known methods such as AMIGO, SIMC, and Cohen–Coon. Both

of these approaches are also clarified in Section 2.5. The performance of all the gained parameters was cross-checked in both rooms over the whole heating period. The analysis is described in detail in Section 2.6.

2.3. Input Data

All the data used for the PI parameter calculations are summarized in Table 1. In this section, only the grey area is described, the rest is tackled in the following sections. Here, the data from [27] were used, where the authors performed temperature setbacks with different lengths in the test building. The air temperature during setbacks with durations of 2 days and 3 days was measured in room 5, where the temperature setpoint was normally kept at 21 °C and during the setbacks was lowered to 18 °C. In the calibrated IDA ICE model, shorter setbacks of 1, 3, 6, 12, and 24 h were simulated using a constant outdoor temperature of 0 °C, with no solar and internal gains. Between the setbacks, the initial temperature of 21 °C was stabilized. Without solar gains, the two test rooms are equivalent and therefore, the PI parameters estimation is based on only one of them.

Table 1. Overview of the input data for the model calculation (grey area) and optimization as well as the methods for getting the proportional–integral (PI) parameters.

Climate	Setpoint	Room	Source	Estimation Basis	Method
Actual	2-3-day (long) setbacks	R5	Measured	Simplified model	Calculation methods + tuning in Matlab
Constant	Shorter setbacks	R5/R6 (equal)	Simulated	Simplified model	Calculation methods + tuning in Matlab
Constant	Infinite/ideal step	R5/R6 (equal)	Simulated	Simplified model	Calculation methods + tuning in Matlab
Estonian TRY	PRBS	R5 and R6	Simulated	Simplified model	Calculation methods
Estonian TRY	Constant	R5 and R6	Simulated	Optimization	GenOpt
Estonian TRY	Variable (price-based)	R5 and R6	Simulated	Optimization	GenOpt

In addition, an ideal-like step test was simulated with the same constant outdoor conditions. A step from no heating to full power heating was performed. The simulation period was prolonged for so long that the stability of the indoor air temperature was achieved both before and after the step. This meant two months in simulation to stabilize at the balance temperature, and one month after the step for reaching a steady state.

Additionally, simulations with Estonian test reference year (TRY) [29] and pseudo-random binary signal (PRBS) as setpoints were used. For the PRBS temperature setpoint, the zero level was set on 18 °C and the maximum level on 24 °C. The simulations were done for two separate weeks, one in March and one in February:

- A sunny week with moderate temperature (19–25.03);
- A cold week with almost no sun (29.01–04.02).

The model fitting was done both on the entire weeks and only on the weekends of these weeks (12 p.m. Friday to 12 p.m. Sunday).

For the optimization (the last two rows in Table 1), the same two weeks of Estonian TRY were used as well as the whole heating period from 1 October to 30 April. The setpoints for the optimization cases are the same as used for the evaluation and are described in Section 2.6.

2.4. Model Fitting

A simplified process model of the system is needed to use most of the PI parameter calculation methods. Based on the generated input data, a first order process model with a time delay was fitted. Therefore, the temperature response of an input step change is

$$\theta(t) = K_p\left(1 - e^{-\frac{t-L}{T}}\right) + \theta(0)e^{-\frac{t-L}{T}} \quad (1)$$

where $\theta(t)$ is room air temperature in °C at time t seconds after the step, $\theta(0)$ is the initial temperature before the step, K_p is the process gain (unitless), T is the time constant, and L is the time delay, both in seconds. The model fitting was performed in Matlab using System Identification Toolbox [30].

2.5. Estimating PI Parameters

The PI parameters K and T_i were estimated, where K is the proportional factor and T_i is the integration time of the integral part of the PI in its ideal form:

$$u(t) = K\left(E + \frac{1}{T_i}\int Edt\right) \quad (2)$$

where u is the control signal (unitless) and E is the difference between the setpoint and measured air temperature in °C that is feedback to the control. For all the cases in Table 1, the PI parameters were estimated by one or more of the following methods:

1. Optimized using GenOpt;
2. Tuned in Matlab/Simulink;
3. Calculated from an applicable simple method.

In the optimization method, the PI parameters were optimized in GenOpt using a hybrid GPS algorithm [31]. The optimization was carried out for the three different periods described previously and two different setpoint profiles, which are also used for the evaluation and are described below in Section 2.6. The objective of the optimization was to minimize the average absolute difference between the setpoint temperature and the simulated temperature.

In the second method, the PI parameters were auto-tuned in Matlab®/Simulink for the previously fitted simplified models (described in Section 2.4). The tuning was performed aiming for a short rise time (speed) and overshoot of no more than 5% of the desired temperature increase.

In the third method, all the models that had been fitted based on the different input data were used to calculate the PI parameters. Three widely known methods—Cohen–Coon, Skogestad IMC (SIMC), and AMIGO—were used for that. The PI parameters K and Ti are calculated according to these methods as follows [32]:

Cohen–Coon (CC): $K = 0.9\cdot\left(1 + 0.092\cdot\frac{\tau}{1-\tau}\right)/$ (3) $Ti = \frac{3.3-3\tau}{1+1.2\tau}L$ (4)

Skogestad IMC (SIMC): $K = T\ /\ \left(2K_pL\right)$ (5) $Ti = \min(T; 8L)$ (6)

AMIGO: $K = \frac{0.15}{K_p} + \left(0.35 - \frac{L\cdot T}{(L+T)^2}\right)\cdot\frac{T}{K_pL}$ (7) $Ti = 0.35L + \frac{13LT^2}{T^2+12LT+7L^2}$ (8)

where Kp, L and T are the parameters from the fitted models with the general representation in Equation (1). The parameters a and τ are unitless parameters:

$$a = \left(K_pL\right)/T \quad (9)$$

$$\tau = L/(L+T) \quad (10)$$

2.6. The Evaluation Tests

All the estimated PI parameter combinations were tested in simulations in both test rooms. The accuracy of the setpoint tracking was assessed on both the constant and variable setpoints. The constant setpoint was chosen to be 21 °C and the variable setpoint was calculated from price data 2017–2018 [33], based on the simple algorithm given in [34] that does not perform the best for their purpose of load shifting but gives us an hourly changing setpoint profile. In the price-based control, the air temperature setpoint is changed hourly between 20, 21, and 24 °C. The lower two levels are meant for comfort and have to be met at all times, the highest level is implemented for load shifting and does not need to be tracked. All evaluations were done for the whole heating period (01 October–30 April). All combinations of PI parameters, both rooms, and both setpoint profiles were evaluated based on:

- The average absolute error (AAE) of the air temperature from the setpoint;
- The heating energy consumption per square meter of the floor area.

For the energy consumption comparison, it is important that no parameter combinations would result in temperatures lower than the given comfort setpoints. In most cases, this was not achieved and, therefore, the setpoints had to be shifted. The goal was to achieve temperatures equal or above the setpoint for at least 97% of the time, as suggested in the thermal comfort standard EN 16798-2 [35]. Based on the initial simulations, cumulative temperature graphs were generated. In the constant setpoint case, the setpoint was shifted exactly as much as the cumulative graph was, below the setpoint at 3% of the time. For the variable setpoints, shifts for both the two 20 °C and 21 °C setpoints were calculated. The 3% of the 20 °C was at 1.3% of the total time and for the 21 °C setpoint at 45.2% of the total heating period length. The maximum of the shifts calculated for these two points was applied to the whole profile.

2.7. Benchmarks

The simulation software IDA ICE's default PI parameter values $K = 0.3$ and $T_i = 300$ s were used for the benchmark simulations. Furthermore, on–off controls with four different dead-band widths were evaluated for the comparison. A modern one with a dead-band of 0.5 °C was used, but also close to ideal versions, with dead-bands of 0.16 °C and 0.05 °C and a conservative one with a 1 °C dead-band, were used as well.

2.8. PI Implementation in IDA ICE and PI Mechanics

As the PI controller can be implemented in various formats, the implementation in IDA ICE is shown in Figure 2. The example code in Figure 2A is modified for the case where error filtering is turned off, the mode is heating, and the conversion unit equals 1. The parameter *tt*, the tracking time, is set to 30 s.

The *hilimit* and *lolimit* are the limits for the PI output signal. In this work, the PI output signal is the fraction of the nominal mass flow to the UFH and is, therefore, limited from 0 to 1. In Figure 2B, an increase in the sample air temperature over the setpoint, i.e., due to solar gains, can be observed. In Figure 2C,D, the calculation of the script can be followed. The lines are colored according to the variable text colors in the script.

In Figure 2C, it can be observed that, even though the temperature is over the setpoint between 3 a.m. and 5 a.m. (Figure 2B), the PI signal is not zero. It only gets to zero when the integral part also decreases so much so that the sum of the integral and error parts is less or equal to zero. Although the *OutSignal* is limited, the negative values of *OutSignalTemp* are still used for the calculation. This enables the effect, which looks like prediction in some cases. This effect is further discussed in Section 3.3.

A.

```
E := SetPoint - Measure;                                    (Figure B)
OutSignalTemp := K * E + K * Integ ;                        (Figure C)
Integ' = E /Ti + (OutSignal - OutSignalTemp)/tt;            (Figure D)
OutSignal = IF OutSignalTemp > hilimit THEN                 (Figure C)
              hilimit
            ELSE_IF OutSignalTemp < lolimit THEN
              lolimit
            ELSE
              OutSignalTemp
            END_IF ;
```

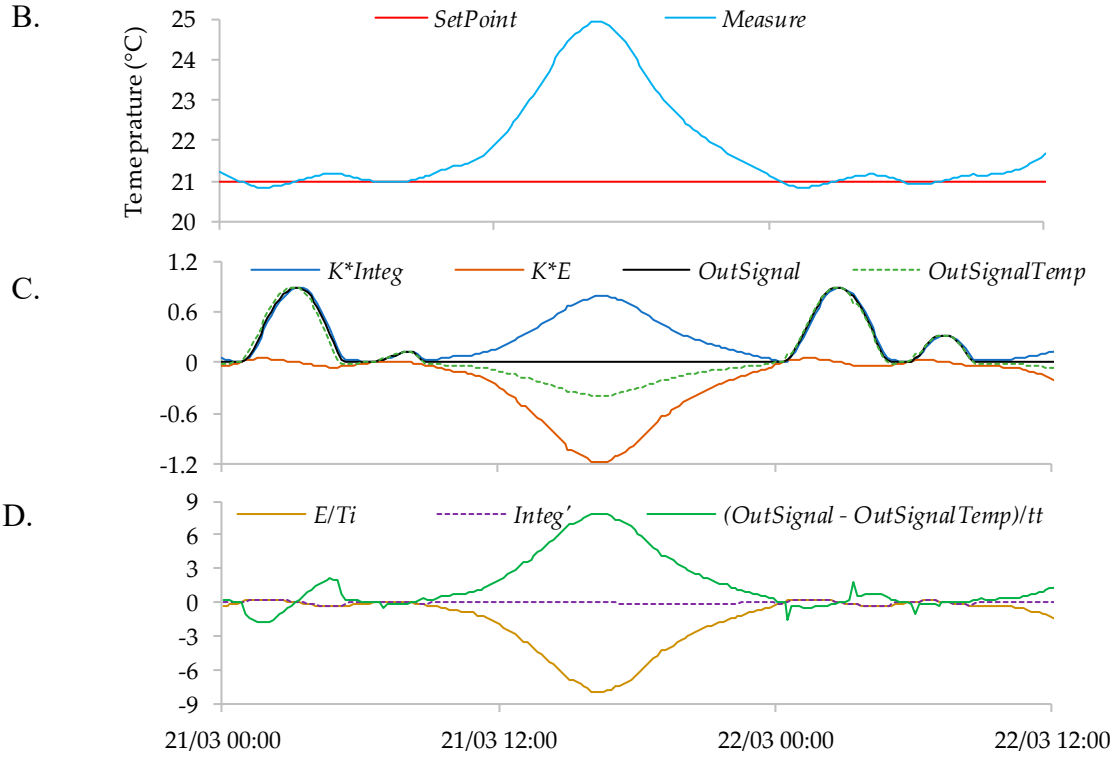

Figure 2. PI implementation in IDA ICE and example signals. In (**A**), variables in the script are colored after each line it is referred where the example signals are visualized. Lines in (**B**–**D**) graphs use the same color-coding.

3. Results

3.1. Found Simplified Models

The simplified model of the system that is needed for the parameter calculation was estimated for 16 different cases. All three parameters of the gained models varied between all cases. The used cases and exact parameter values are included in Table 2 with parameter values also visualized in Figure 3. The process gain (K_p) has two clearly different orders and altogether three different levels. The values were around 1 for all cases where the PRBS signal was used as the setpoint and were much larger for

other cases. For the ideal step and measured setbacks, the K_p value was around 20, for all other setback cases, around 40.

Table 2. List of all used models and their parameters.

Based on Room	Model Number	Model Group	Model Source	K_p	L (Seconds)	T (Seconds)
R5 & R6	1	Longer step	Ideal step	21.842	476	27,892
	2	Setbacks	24-h setback at 0 °C	41.063	141.12	23,652
	3	Setbacks	12-h setback at 0 °C	42.649	410.58	30,141
	4	Setbacks	6-h setback at 0 °C	44.717	156.96	38,648
	5	Setbacks	3-h setback at 0 °C	42.664	9.66	35,191
	6	Setbacks	1-h setback at 0 °C	41.446	3.9	42,130
R5	7	Longer step	2-day measured setback	24.256	720	33,720
	8	Longer step	3-day measured setback	21.472	780	41,820
	9	PRBS sL	2-day PRBS in February	1.0123	218.4	27,152
	10	PRBS sL	1-week PRBS in February	1.03	286.8	50,122
	11	PRBS lL	2-day PRBS in March	1.0555	2034	48,950
	12	PRBS lL	1-week PRBS in March	1.0599	2226.6	51,845
R6	13	PRBS sL	2-day PRBS in February	1.03	25.8	17,237
	14	PRBS sL	1-week PRBS in February	1.042	12.6	34,930
	15	PRBS lL	2-day PRBS in March	1.0973	3996	41,990
	16	PRBS lL	1-week PRBS in March	1.1035	50,084	4737

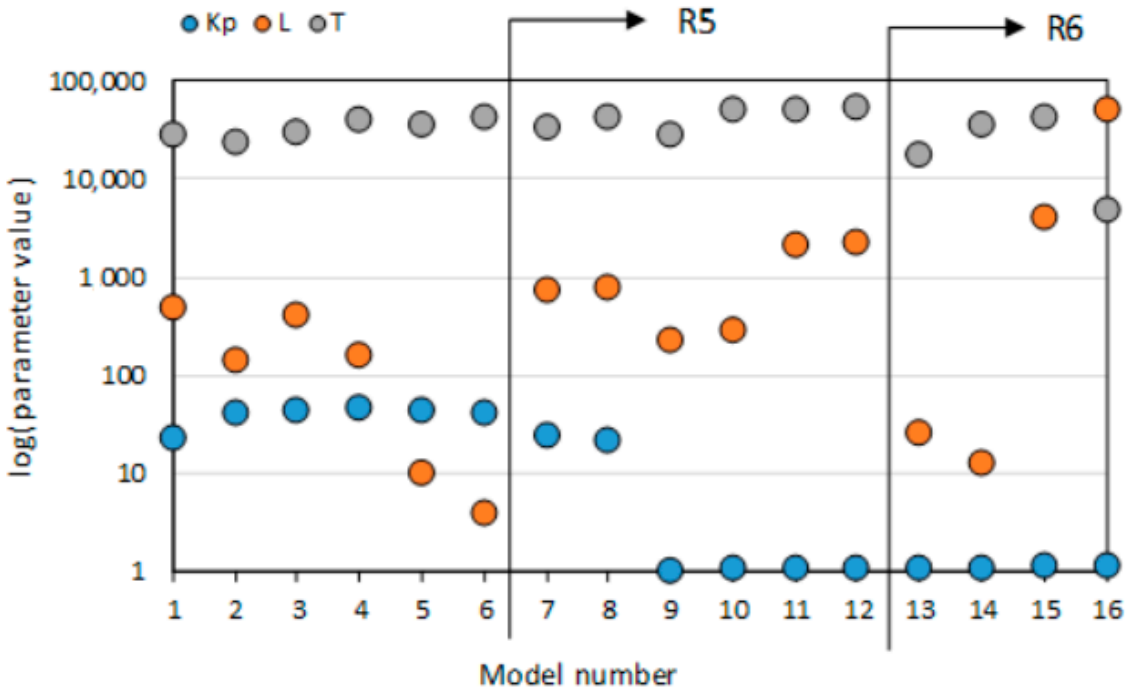

Figure 3. Log-value of all model parameters shown in Table 2.

The time delay (L) values for the PRBS cases had around a 100 times difference between the March week and February week values in R5, and the same difference was larger than 1000 times in R6, the southern room with more solar gains. L was smaller than 10 s for the two shortest setbacks, between 10 and 30 s for the February PRBS tests in R6, and larger than 100 in all other cases. There was

ranging from 140 to 4000 (around 2 m to 1 h) and in one case (1-week PRBS in March for R6, model 16) it was over 50,000 s (around 14 h).

The T values varied least of the parameters, i.e., between 10,000 and 100,000 s (between around 4 and 15 h). Only in the same model 16 case, where an extra-large L value occurred, the T value was a lot lower at a bit less than 5000. So exceptionally, for this model, L is larger than T.

Based on mostly the K_p and L values, the models are divided into four groups, shown in Table 2. The setbacks and longer step groups are self-evident from above. The PRBS models are divided into models with a short L (PRBS sL) and a long L (PRBS lL). These groups will be used below for visualization.

3.2. Identified PI Parameters

In total, 68 PI parameter value pairs were obtained. All the parameter values are included in Appendix A, Table A1. However, all the parameter combinations are also visualized in Figure 4a, where each point on the graph is a parameter combination. The scales are the logarithms of the parameter values with base 10. The graphs in Figures 4b and 5 follow the same logic. In Figure 4a, the parameter estimation method is shown by the marker shape and the model group is shown by the marker color. In the logarithmic scales, the tendency in the parameter estimation results seems to be roughly linear, so the lower the integration time the higher the proportional gain.

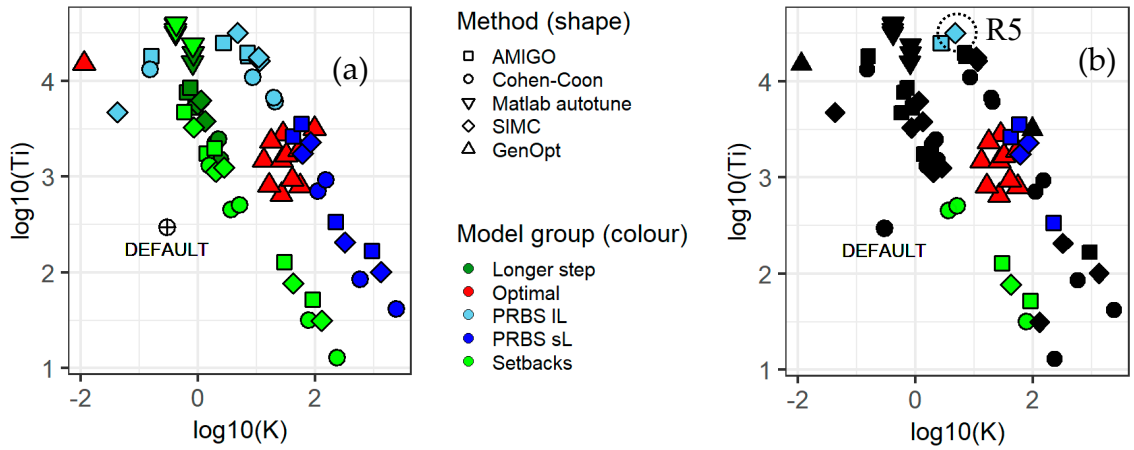

Figure 4. All PI parameter value pairs (*K, Ti*) on log-valued axes colored based on the method, in (**a**) the default black circle with cross is the PI parameters pair used in IDA ICE by default, in (**b**) the black points are the ones that would not result in acceptable temperatures for R6 without setpoint shifting.

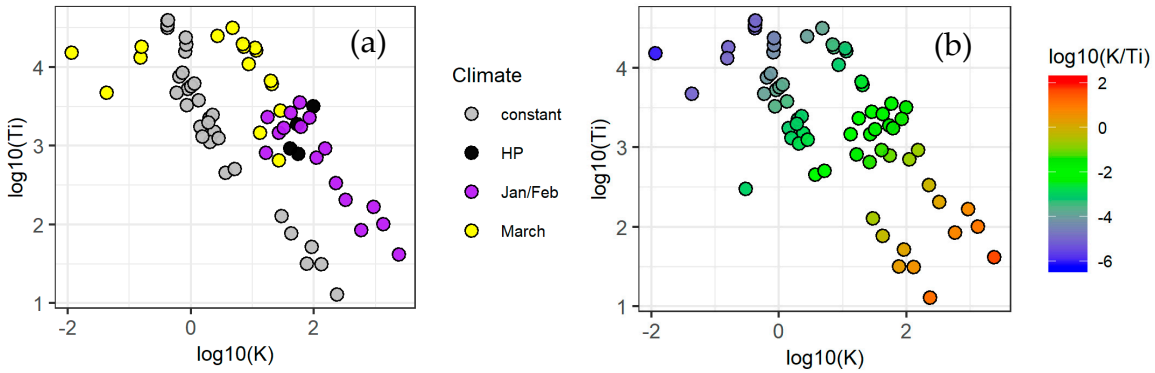

Figure 5. Graph (**a**) shows the underlying climate data and graph (**b**) shows the log-ratio values of all the PI parameter pairs. In (**a**), the constant climate is at 0 °C with no solar radiation, HP stands for heating period and all the dates are covered in Section 2.

For the very small proportional gain, the integration time varies significantly from this otherwise linear behavior in the log10-log10 scale. The reason for this is depicted partly in Figure 5a. As can be seen, this covers the four cases calculated or optimized for March. Actually, these were all achieved for Room 6. This means that the solar peaks have been severe and almost no heating was needed. Therefore, these cases resulted in obscure parameters.

The clear separation between parameters is evident. The two sets of parameters with both blue and red (optimal) results made up one group and both green ones the other. This is also the difference in outdoor conditions, as can be seen in Figure 5a. The first group was generated at dynamic outdoor temperatures and realistic solar irradiation, while the second group bordered constant outdoor temperatures and no solar radiation. Here, also the separation between the March and Jan/Feb periods is clear, so it can be assumed that more solar gains causes the K parameter to be smaller and T_i to be longer. For the optimal cases, the combinations closer to the blue ones are optimized for the variable setpoint, the lower values for the constant setpoint.

In Figure 4b, the parameter combinations, which do not achieve the needed setpoints in Room 6 for at least 97% of the time (with a slack of 0.05 °C), are colored black. Both the one constant and two variable setpoint levels are checked and the coloring shows if any of the three are violated. If the graph would be for R5, all of the points, except the one with a dashed circle around it, would be black. This means that only one parameter combination would achieve the required temperatures in R5, if the setpoints were not shifted, as it was described in Section 2.6.

In Figure 5b, all the K-T_i pairs are colored by the log10 (K/T_i) value. This logarithm is further used for describing the pairs, as this is a clear indicator whether the pair is in the lower right or upper left corner of the log10-log10 graph.

3.3. Setpoint Temperature Tracking and PI Output Signal Behaviour

Each parameter combination results in different air temperature profiles and PI output signal profiles. There are four examples of the temperature and PI output profile combinations shown in Figure 6 for the constant setpoint cases and in Figure 7 for the variable setpoint cases in Room 6. In both figures, the Jan/Feb week is depicted on the left and the March week on the right. The parameter combinations are chosen as the ones with minimum and maximum log10 ratios of the parameters, the IDA ICE default combination, and the one which resulted in optimal energy consumption (see Section 3.5). The combinations are ordered by the log10 ratio of the parameters with the minimum ratio at the top and the maximum ratio at the bottom. The IDA ICE default combination is the second (0.3/300) and the optimal is the third from the top (18/2300). Here, the parameter values were rounded to two significant numbers.

In the first column of Figure 6, most of the controllers show results that suggest maintaining a constant setpoint in the situation with no solar gains is an easy task. The small fluctuations are largest when a very small proportional gain (K = 0.012 in Figure 6a) with a large integration time is applied. This controller changes the signal too slowly, as its PI output signal in black shows. The signal stays almost constant throughout the day and even throughout the week. Due to the same effect, temperatures drop below the constant setpoint in March in Figure 6b and the setpoint tracking is poor in the variable cases. The level at which the signal is constant depends on the season, as there is a clear difference between February and March.

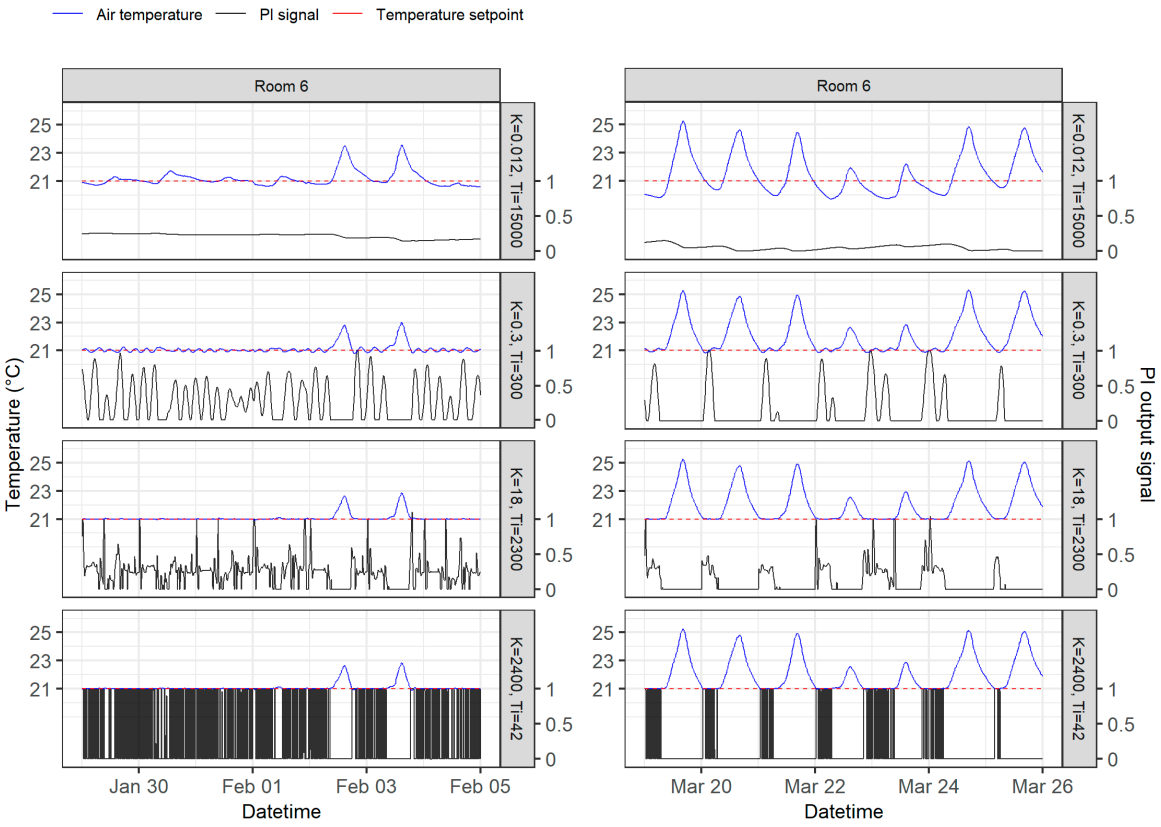

Figure 6. Air temperatures and PI output signals for the constant setpoint case during one week in January/February (**left**), and in a week in March (**right**) for the chosen four pairs of parameters.

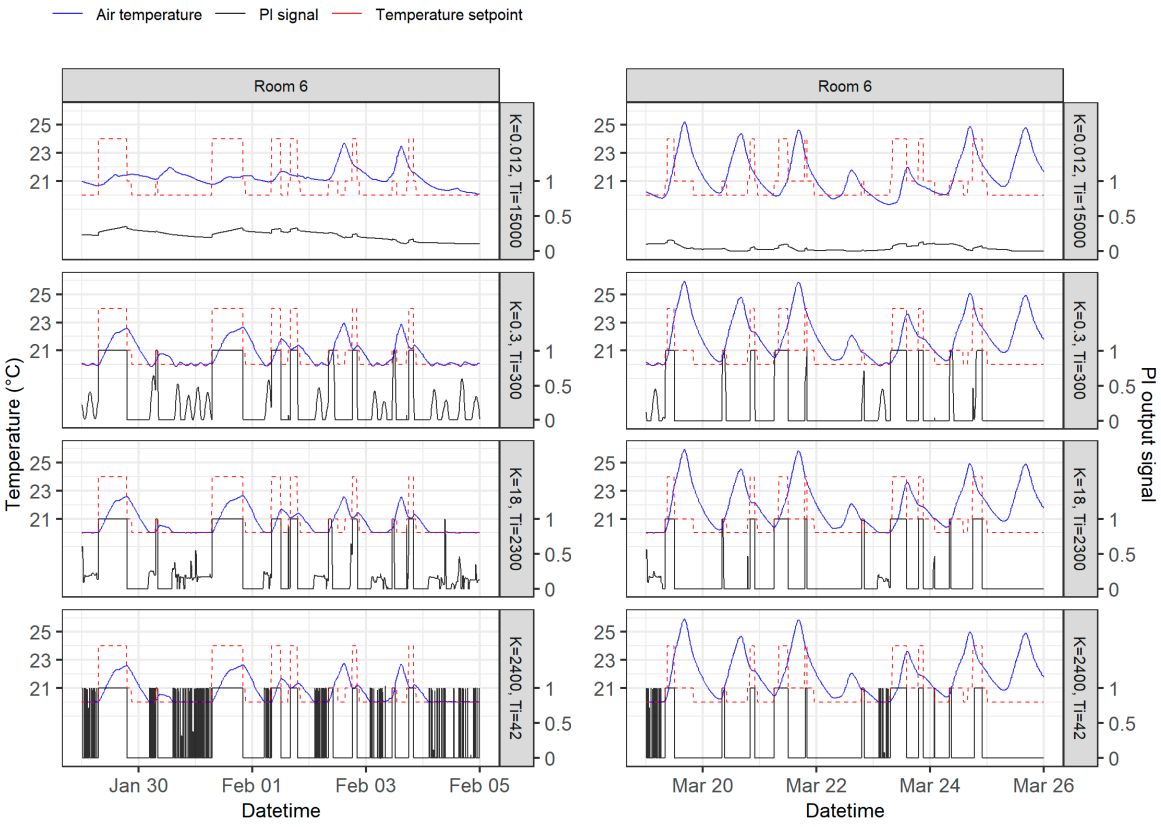

Figure 7. Air temperatures and PI output signals for the variable setpoint case during one week in January/February (**left**), and in a week in March (**right**) for the chosen four pairs of parameters.

The constant setpoint cases in Figure 6 show that 2400/42 manages to maintain the constant setpoint the best. However, there is no significant difference for the variable setpoint cases. However, the PI output signal in the same case changes most rapidly. Both a large proportional gain and relatively small integration time contribute to this. Such switching reduces the life span of most of the devices, so this would not be acceptable in practice. For the case with also a large proportional gain but with a large integration time as well (18/2300), the signal is a bit smoother. In the long integration time cases, the heating starts earlier and stops sooner than for the shorter integration time. It can be observed that the PI signal turns on before the temperature lowers below the setpoint generating a prediction effect. This is especially clear for 18/2300 during the March week.

The variable setpoint cases in February in Figure 7's first column show that in cold weather with no solar peaks, the 24 °C setpoint peaks were not reached due to the short duration of the setpoint increase. Therefore, setpoint tracking during high setpoints is clearly not good but is also not required. However, the PI signal is 1 during these times, which means the heater is fully on as is the aim for load shifting. In this figure, again controllers 18/2300 and 2400/42 both maintain the lower setpoint well. However, the latter is switching on and off often and has almost no other state. In March, the solar peaks govern the temperatures. However, the second column of Figure 7 shows that the heating is turned on as well.

All the cumulative profiles over the heating period are shown in Figure 8. For the PI signal, only R6 is shown as the profiles look very similar for the two rooms. The switching behavior indicated before is clearly dependent on the log10 ratio of the PI parameters. The higher the ratio, the more abrupt the changes, as the cumulative graph indicates behaviors close to on–off signals. As shown in Figure 9, a zoom-in on R6's constant setpoint graph, the higher temperatures at the high-temperature end are clearly dependent on the *Ti* value. The low-temperature end seems to be more dependent on the *K* value. Therefore, the energy consumption of the parameter combination is mostly dependent on the *K* value and avoiding over-heating at the disturbances is more dependent on the *Ti* value. This effect was also observed in the analysis.

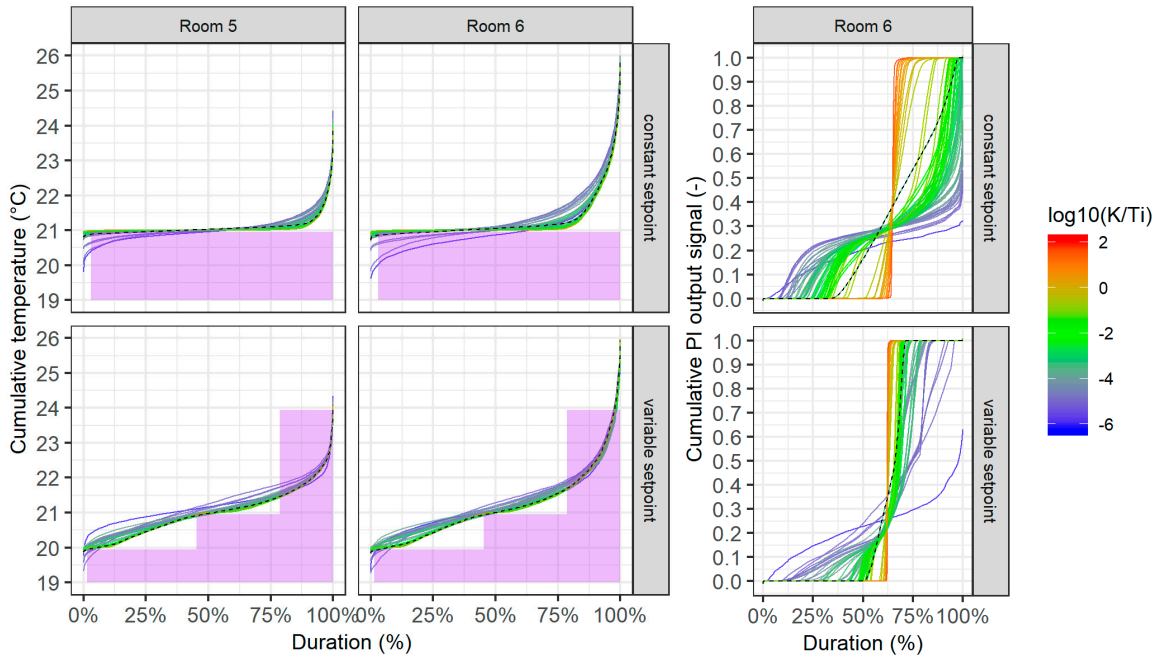

Figure 8. Duration curves over the heating period for temperatures on the left and PI output signals on the right. The purple indicates the temperatures below the setpoint and the black dashed line shows the results of the IDA ICE default parameters.

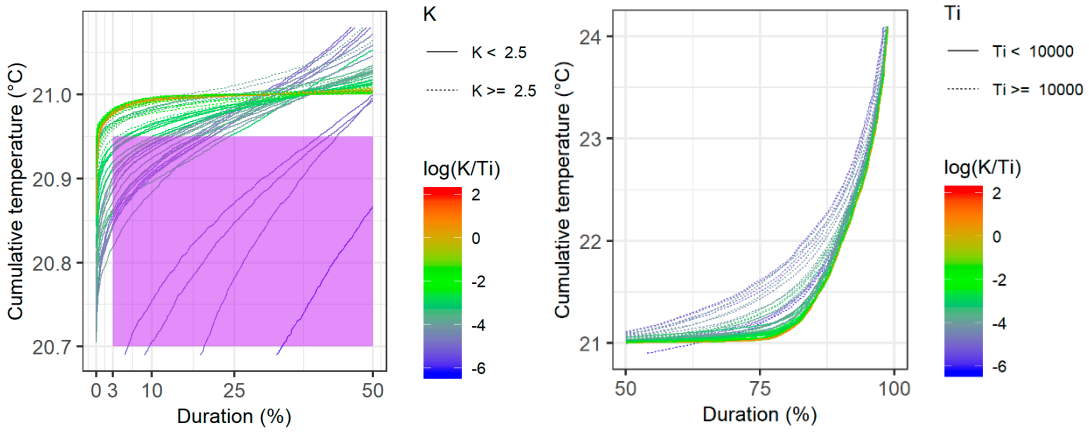

Figure 9. (**Left**): Zoom-in on Figure 8's lower temperature end of the constant temperature graph of R6; (**right**): Zoom-in on the temperature end of the same graph.

3.4. Setpoint Shifting

It is clear, that some of the parameter combinations did not achieve the required temperature setpoint and some resulted in higher temperatures above the setpoint. Especially at the high temperature end, there was also a clear difference between rooms R5 and R6, as can be seen from Figure 8. This was caused by the room orientations as the R6 faces south-west and gets more solar gains than the north-west orientated R5. As declared in Section 2.6, the setpoints were shifted for all cases in the way that temperatures would reach the required setpoint for at least 97% of the time. The shift values were different for R5 and R6 as well as for the constant and variable setpoint cases. As a result, all temperatures reached the given setpoints at around 95–97% of the heating period. This accuracy was considered satisfactory. The shifts are shown together with the energy consumption evaluation in Figure 10.

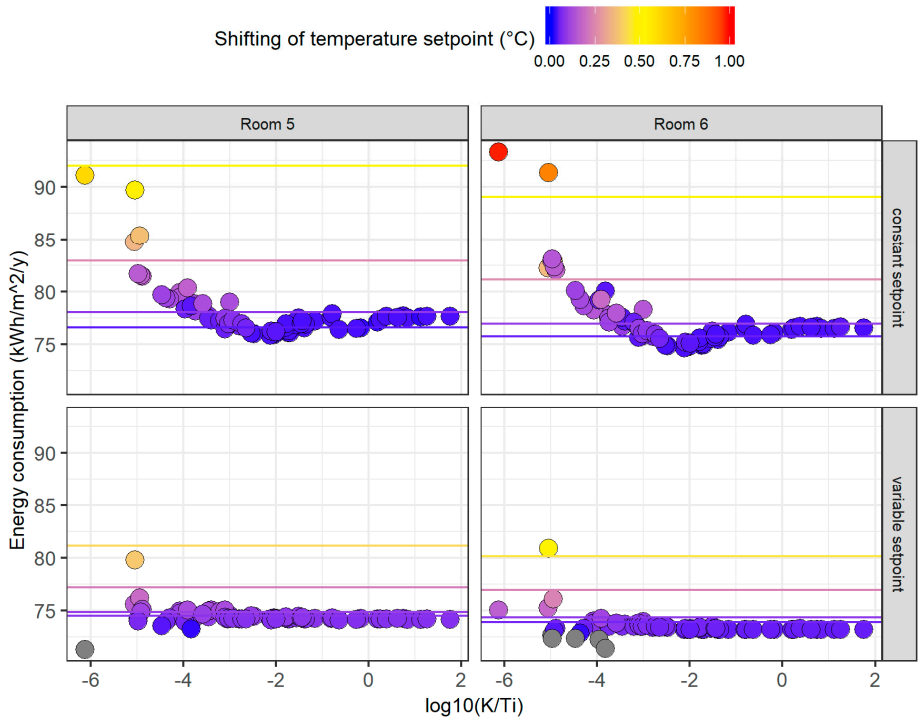

Figure 10. Influence of the log10 of the PI parameters ratio *K*/*Ti* on energy consumption in the 10.4 m^2 rooms; color-scale shows the setpoint shift; the grey values are below 0 which means that the temperature setpoints have been decreased. The horizontal lines depict the setpoint shifts and energy consumption of the on–off cases with different dead-bands.

3.5. Energy Performance and Total Setpoint Tracking Accuracy

The energy consumption results after setpoint shifting are shown in Figures 10 and 11. It is clear that the variable setpoint cases consumed less energy. This is because the average room temperatures were lower. The setpoints were also higher than the constant cases in some periods but coincidentally the higher setpoint temperatures often occurred during the day and the lower setpoints occurred during the night, so this does not influence heating energy use much. Also, the high setpoints were not actually reached. In the constant temperature cases, a clear optimum emerged between the log10 ratio of −3 and −1. This means that in optimal cases, the K value was 10 to 1000 times smaller than *Ti*.

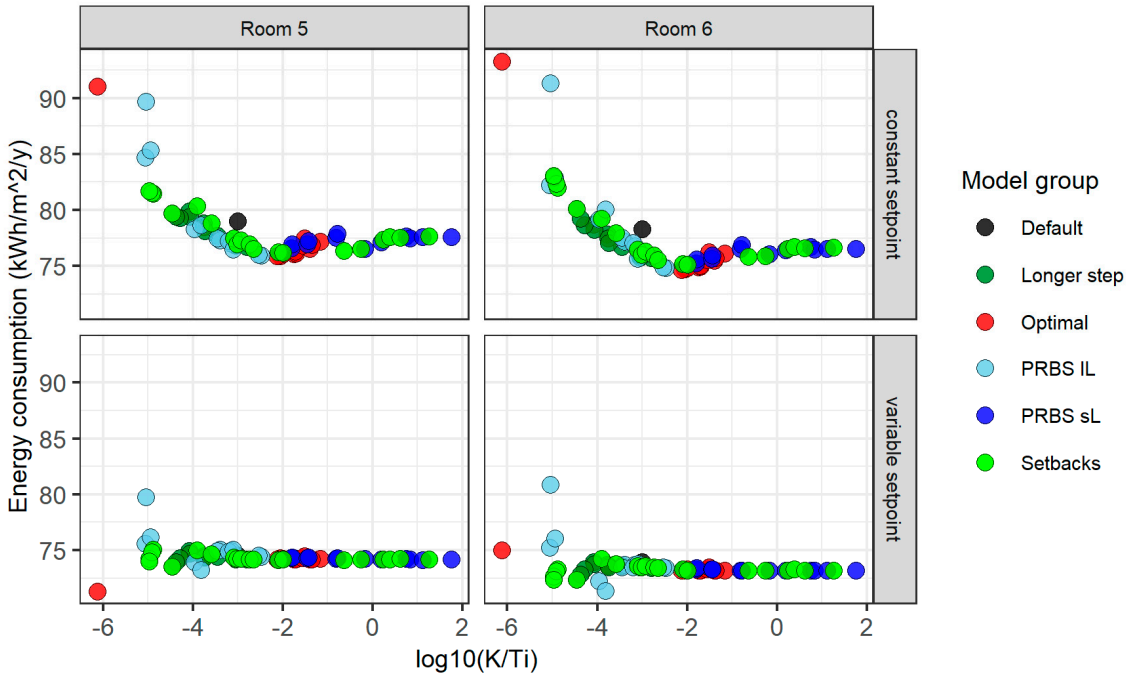

Figure 11. Influence of the log10 of the PI parameters ratio *K*/*Ti* on energy consumption; colors visualize the underlying model group.

The horizontal lines in Figure 10 represent the shifted energy performance at the benchmark for the on–off cases with different dead-bands. From top to bottom (yellow to blue) the corresponding dead-bands are 1 K, 0.5 K, 0.16 K, and 0.05 K. The optimal PI parameter combinations result in a lower energy consumption than even the lowest of the lines with an unrealistically small dead-band. The commonly used dead-band of 0.5 K consumes 2–3 kWh/m^2/year more energy than the PI cases for the variable setpoint. For the constant setpoint, the lowest PI results are up to 7 kWh/m^2/year or 9% lower than for the on–off with a 0.5 K dead-band, which, for example, in R6 is at 81 kWh/m^2/year. Omitting the extreme poorly performing cases, the total variation in energy consumption is more than 10 kWh/m^2/year or 12% in the constant setpoint case.

Figure 11 shows the same data colored by the model group. The IDA ICE default parameter is at one edge of the optimum range with exactly 1000 times difference. The energy consumption is already around 5 kWh/m^2/year or 5% higher on that edge compared with the optimal case. The parameters optimized for setpoint tracking are also close to an optimal energy consumption. The PRBS sL group performs well almost in all cases but not optimally, while in all other groups some combinations perform poorly. The optimal range of parameters is shown in detail in Table 3. Most of the optimal values were calculated using TRY climate data but the methods varied.

Table 3. Optimal parameter combinations from log10 ratio from −3 (excluded) to −1. Ordered in increasing energy consumption values for the R6 constant setpoint.

K	*Ti*	Model	Method	Climate	Setpoint	Room	Total Length
18	2300	-	GenOpt	TRY, Jan/Feb week	variable	R6	Inf
13	1500	-	GenOpt	TRY, March week	constant	R5	Inf
28	2800	-	GenOpt	TRY, March week	variable	R5	Inf
21	6200	11	Cohen-Coon	TRY, March weekend	PRBS	R5	2 days
20	6700	12	Cohen-Coon	TRY, March week	PRBS	R5	7 days
27	1500	-	GenOpt	TRY, Jan/Feb week	constant	R5	Inf
16	820	-	GenOpt	TRY, Jan/Feb week	constant	R6	Inf
32	1700	-	GenOpt	TRY, Jan/Feb week	variable	R5	Inf
5.2	510	4	Cohen-Coon	Const	6-h setback	equal	1.5 days
3.7	460	2	Cohen-Coon	Const	24-h setback	equal	6 days
42	2700	9	AMIGO	TRY, Jan/Feb weekend	PRBS	equal	2 days
27	650	-	GenOpt	TRY, March week	constant	R6	Inf
54	1900	-	GenOpt	TRY, heating period	variable	R5	Inf
2.8	1300	4	SIMC	Const	6-h setback	equal	1.5 days
59	3600	10	AMIGO	TRY, Jan/Feb week	PRBS	R5	7 days
61	1800	9	SIMC	TRY, Jan/Feb weekend	PRBS	R5	2 days
41	930	-	GenOpt	TRY, heating period	constant	R6	Inf
2.4	1500	1	Cohen-Coon	Const	Ideal step	equal	60 days
2.0	1100	2	SIMC	Const	24-h setback	equal	6 days
85	2300	10	SIMC	TRY, Jan/Feb week	PRBS	R5	7 days
55	800	-	GenOpt	TRY, heating period	constant	R5	Inf
98	3200	-	GenOpt	TRY, heating period	variable	R6	Inf
1.6	1300	3	Cohen-Coon	Const	12-h setback	equal	3 days

The AAE of the temperatures for rooms R5 and R6 are shown in Figure 12. The AAE is clearly dependent on the room and setpoint but not on the parameter combination. The AAE is constantly at 0.5 K for R5 and around 0.7 for R6 in the variable setpoint cases. The accuracy here depends mostly on the solar gains. For the constant setpoint case, the optimal region is everything, with a *Ti* lower than 10^4 and a *K* higher than $10^{0.5}$. The error is around 0.2 K for all the simulations in R5, for R6 the error ranges from 0.25 to 0.6 K, and in extreme cases to 1 K.

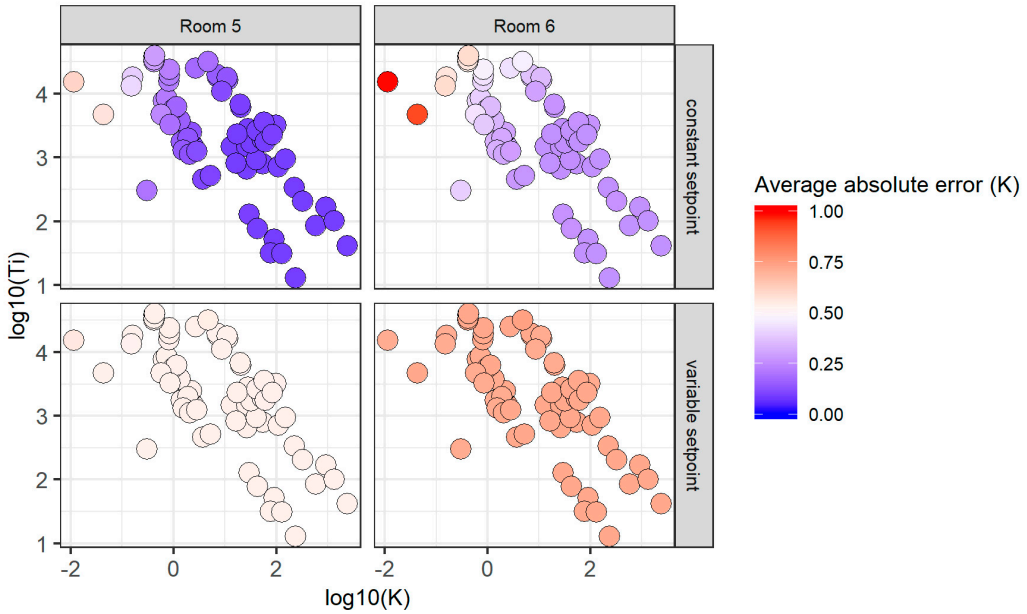

Figure 12. Absolute average error (AAE) of the air temperature compared to the setpoint.

4. Discussion

Different PI parameter estimation methods were applied on various periods and control profiles. An optimal region of the parameter ratio was determined where the energy consumption was the lowest. Half of the parameter combinations in the optimal region for energy consumption were found via GenOpt, although they were optimized for the minimal temperature setpoint tracking error. Although most reliably well-performing, this approach is not always suitable in practice as it requires an advanced model of the building. Therefore, it is practical that the other half of the parameter combinations in the optimal region were found using only short tests and simple calculations.

For all these other methods, simplified models were identified. In the optimal region, all the tested simplified methods were represented: Cohen–Coon, AMIGO, and SIMC. The results tuned in Matlab were not represented, probably due to the chosen goal being speed for that methodology. The models underlying these calculations were obtained from the week or weekend pseudo-random temperature setpoint (PRBS) data or setbacks of 6, 12, or 24 h. It is clear that the longer the setback, the easier it is to identify a simple model on it. This is probably the reason why the 1- and 3-h setbacks resulted in less desirable parameters. Still, conducting 24-h setbacks would probably not be comfortable for the occupants. Therefore, it is beneficial that 6-h setbacks could suffice. For example, these could be conducted during the night when the outdoor conditions are less variable with no solar gains. The suitable PRBS cases included both the January and March data, indicating that it is possible to get quality parameters in various weather conditions.

The optimal parameter combinations resulted in an annual heating energy reduction of up to 9% or 7 kWh/m^2/year. The comparison of heat emitters and controllers in the European standard room shows similar results with 5% to 10% savings for the PI controlled UFH compared with the on–off control [20]. This does not compare to the 32% achieved for radiators in [23], however, the actual difference is difficult to compare as the baselines are different. The reduction of 7 kWh/m^2/year here can be seen as highly significant as this can be achieved with only parameter correction, which does not require intensive computation when the simple tests are applied. Accounting for the more expensive thermostat head with variable parameters option, the payback time of this change is around 5 years. This saving can be achieved without setpoint reductions, which means no penalty on comfort. On the contrary, due to less fluctuation, comfort could even improve.

The methodology used here could be applied in any UFH system. In public and office buildings, a detailed model often exists and optimization of the parameters could be possible. Due to the large floor areas in these buildings, the absolute savings could be significant compared with the on–off control. Even more evident would be the saving in outdoor UFH systems installed under garage runways or stadiums to keep them clear from ice and snow.

Evidently, the parameter value results apply to the studied building, and future research can determine possible variation of the parameters in buildings with a smaller or higher thermal mass, insulation level, and maximum heating power. However, the wide range of well-performing parameter combinations and the fact that the suitable region is the same for both the north and south facing rooms provides an indication that the parameters from this region could be suited to different buildings as well. This should be confirmed by future studies on the subject.

5. Conclusions

Several combinations of the input data and PI parameter estimation methods were applied with the aim to improve UHF temperature control, resulting in 68 different PI parameter combinations. Based on the results and discussion above, most importantly concluded is that:

- For the first time in the scientific literature, it is shown that UFH can operate with determined PI parameters similar to ideal control;
- A performance close to optimal could also be achieved by parameters achieved from shorter tests, e.g., weekend pseudo-random setpoints, and 6- to 24-h setbacks which were shown to be suitable;
- The optimal PI parameters improved the room temperature control accuracy considerably, and that the results show that the UFH PI control with the correct parameters started to work in a predictive fashion and the resulting room temperature curves were practically ideal;
- The optimal PI parameters reduced the energy consumption for heating by up to 9% (7 kWh/m^2/year) in comparison with the on–off control (at around 80 kWh/m^2/year) and by 5% in comparison with the default PI parameters;
- The variation amplitude of the heating energy needed using different estimated (not random) parameters was more than 15 kWh/m^2/year for the constant setpoint, which stresses the importance of having the correct PI parameters;
- The optimal PI parameters included combinations with log10 *(K/Ti)* between −3 and −1, in these combinations, the proportional gain *K* ranged from 2 to 100 and the integration time *Ti* from 500 to 6700 s, and thus higher gain and longer integration time values than are conventionally used are recommended;
- For the variable setpoint, using the PI control had a similar effect to decreasing the dead-band and the variation in the PI parameters did not have a significant further effect on the energy consumption, except for when they were extremely poorly tuned;
- The average absolute error for the air temperatures from the setpoint was well below 0.5 K for the constant setpoints, but above for the variable setpoints.

Author Contributions: Conceptualization, T.M.K. and M.T. and J.K.; methodology, T.M.K. and M.T. and J.K.; software, T.M.K.; validation, T.M.K.; formal analysis, T.M.K.; investigation, T.M.K.; resources, T.M.K. and M.T. and J.K.; data curation, T.M.K.; writing—original draft preparation, T.M.K.; writing—review and editing, M.T. and J.K.; visualization, T.M.K.; supervision, M.T. and J.K.; project administration, J.K. and M.T.; funding acquisition, J.K. and M.T. All authors have read and agreed to the published version of the manuscript.

Funding: This research was supported by the Estonian Centre of Excellence in Zero Energy and Resource Efficient Smart Buildings and Districts, ZEBE (grant No. 2014-2020.4.01.15-0016) and the programme Mobilitas Pluss (Grant No—2014-2020.4.01.16-0024, MOBTP88) funded by the European Regional Development Fund, by the Estonian Research Council (grant No. PSG409) and by the European Commission through the H2020 project Finest Twins (grant No. 856602).

Conflicts of Interest: The authors declare no conflict of interest.

Appendix A

Table A1. All obtained parameter values, which were not already shown in Table 3, sorted by log10 ratio from largest to smallest.

K	*Ti* (s)	Model	Method	Climate	Setpoint	Room	Total Length (Days)
2400	42	14	Cohen-Coon	TRY, Jan/Feb week	PRBS	R6	7
235	13	6	Cohen-Coon	Const	1-h setback	equal	0.25
1300	100	14	SIMC	TRY, Jan/Feb week	PRBS	R6	7
580	85	13	Cohen-Coon	TRY, Jan/Feb weekend	PRBS	R6	2
930	170	14	AMIGO	TRY, Jan/Feb week	PRBS	R6	7
130	31	6	SIMC	Const	1-h setback	equal	0.25
77	32	5	Cohen-Coon	Const	3-h setback	equal	0.75
91	52	6	AMIGO	Const	1-h setback	equal	0.25
320	210	13	SIMC	TRY, Jan/Feb weekend	PRBS	R6	2
230	340	13	AMIGO	TRY, Jan/Feb weekend	PRBS	R6	2
43	77	5	SIMC	Const	3-h setback	equal	0.75
30	130	5	AMIGO	Const	3-h setback	equal	0.75
150	940	10	Cohen-Coon	TRY, Jan/Feb week	PRBS	R5	7
110	710	9	Cohen-Coon	TRY, Jan/Feb weekend	PRBS	R5	2
1.9	2000	4	AMIGO	Const	6-h setback	equal	1.5
2.3	2500	8	Cohen-Coon	Actual	3-day measured	R5	3
2	2300	7	Cohen-Coon	Actual	2-day measured	R5	2
1.4	1800	2	AMIGO	Const	24-h setback	equal	6
8.7	11,000	15	Cohen-Coon	TRY, March weekend	PRBS	R6	2
11	16,000	11	SIMC	TRY, March weekend	PRBS	R5	2
11	18,000	12	SIMC	TRY, March week	PRBS	R5	7
7.2	18,000	11	AMIGO	TRY, March weekend	PRBS	R5	2
7	20,000	12	AMIGO	TRY, March week	PRBS	R5	7
1.3	3800	1	SIMC	Const	Ideal step	equal	60
0.9	3300	3	SIMC	Const	12-h setback	equal	3
1.1	6200	8	SIMC	Actual	3-day measured	R5	3
1	5800	7	SIMC	Actual	2-day measured	R5	2
0.9	5300	1	AMIGO	Const	Ideal step	equal	60
4.8	32,000	15	SIMC	TRY, March weekend	PRBS	R6	2
0.6	4700	3	AMIGO	Const	12-h setback	equal	3
2.7	25000	15	AMIGO	TRY, March weekend	PRBS	R6	2
0.7	8500	8	AMIGO	Actual	3-day measured	R5	3
0.6	7700	7	AMIGO	Actual	2-day measured	R5	2
0.81	16,000	1	tuned in Matlab	Const	Ideal step	equal	60
0.83	20,000	7	tuned in Matlab	Actual	2-day measured	R5	2
0.82	24,000	8	tuned in Matlab	Actual	3-day measured	R5	3
0.82	24,000	2	tuned in Matlab	Const	24-h setback	equal	6
0.41	32,000	3	tuned in Matlab	Const	12-h setback	equal	3
0.41	34,000	5	tuned in Matlab	Const	3-h setback	equal	0.75
0.15	13,000	16	Cohen-Coon	TRY, March week	PRBS	R6	7
0.43	40,000	6	tuned in Matlab	Const	1-h setback	equal	0.25
0.41	39,000	4	tuned in Matlab	Const	6-h setback	equal	1.5
0.043	4700	16	SIMC	TRY, March week	PRBS	R6	7
0.16	18,000	16	AMIGO	TRY, March week	PRBS	R6	7
0.012	15,000	-	genopt	TRY, March week	variable	R6	Inf

References

1. Salata, F.; Golasi, I.; Domestico, U.; Banditelli, M.; Basso, G.L.; Nastasi, B.; Vollaro, A.D.L. Heading towards the nZEB through CHP+HP systems. A comparison between retrofit solutions able to increase the energy performance for the heating and domestic hot water production in residential buildings. *Energy Convers. Manag.* **2017**, *138*, 61–76. [CrossRef]
2. Becchio, C.; Dabbene, P.; Fabrizio, E.; Monetti, V.; Filippi, M. Cost optimality assessment of a single family house: Building and technical systems solutions for the nZEB target. *Energy Build.* **2015**, *90*, 173–187. [CrossRef]
3. Péan, T.; Salom, J.; Castello, R.C. Review of control strategies for improving the energy flexibility provided by heat pump systems in buildings. *J. Process. Control.* **2019**, *74*, 35–49. [CrossRef]
4. EU Buildings Factsheets. Available online: https://ec.europa.eu/energy/eu-buildings-factsheets_en (accessed on 20 April 2020).
5. Thonipara, A.; Runst, P.; Ochsner, C.; Bizer, K. Energy efficiency of residential buildings in the European Union—An exploratory analysis of cross-country consumption patterns. *Energy Policy* **2019**, *129*, 1156–1167. [CrossRef]
6. Kummert, M.; Andre, P.; Nicolas, J. Optimal heating control in a passive solar commercial building. *Sol. Energy* **2001**, *69*, 103–116. [CrossRef]
7. Wolisz, H.; Kull, T.M.; Müller, D.; Kurnitski, J. Self-learning model predictive control for dynamic activation of structural thermal mass in residential buildings. *Energy Build.* **2020**, *207*, 109542. [CrossRef]
8. Astrom, K.; Hägglund, T. The future of PID control. *Control. Eng. Pr.* **2001**, *9*, 1163–1175. [CrossRef]
9. Dounis, A.I.; Caraiscos, C. Advanced control systems engineering for energy and comfort management in a building environment—A review. *Renew. Sustain. Energy Rev.* **2009**, *13*, 1246–1261. [CrossRef]
10. Royapoor, M.; Antony, A.; Roskilly, T. A review of building climate and plant controls, and a survey of industry perspectives. *Energy Build.* **2018**, *158*, 453–465. [CrossRef]
11. Salsbury, T.I. A SURVEY OF CONTROL TECHNOLOGIES IN THE BUILDING AUTOMATION INDUSTRY. *IFAC Proc. Vol.* **2005**, *38*, 90–100. [CrossRef]
12. Rodríguez-Rodríguez, I.; González-Vidal, A.; González, A.R.; Izquierdo, M.A.Z. Commissioning of the Controlled and Automatized Testing Facility for Human Behavior and Control (CASITA). *Sensors* **2018**, *18*, 2829. [CrossRef] [PubMed]
13. Seidel, S.; Haufe, J.; Majetta, K.; Blochwitz, T.; Liebold, E.; Hintzen, U.; Klostermann, V.; Clauß, C. Modelica based Design and Optimisation of Control Systems for Solar Heat Systems and Low Energy Buildings. In Proceedings of the 11th International Modelica Conference, Versailles, France, 21–23 September 2015; Volume 118, pp. 401–410.
14. Astrom, K.; Hägglund, T.; Wallenborg, A. Automatic tuning of a digital controller. In Proceedings of the 4th IFAC Symposium on Adaptive Systems in Control and Signal, Grenoble, France, 1–3 July 1992; Volume 25, pp. 285–290. [CrossRef]
15. Wang, Y.-G.; Shi, Z.-G.; Cai, W.-J. PID autotuner and its application in HVAC systems. In Proceedings of the 2001 American Control Conference. (Cat. No.01CH37148), Arlington, VA, USA, 25–27 June 2001; pp. 2192–2196. [CrossRef]
16. Bi, Q.; Cai, W.-J.; Wang, Q.-G.; Hang, C.-C.; Lee, E.-L.; Sun, Y.; Liu, K.-D.; Zhang, Y.; Zou, B. Advanced controller auto-tuning and its application in HVAC systems. *Control. Eng. Pr.* **2000**, *8*, 633–644. [CrossRef]
17. Ferrarini, L.; Rastegarpour, S.; Petretti, A. An Adaptive Underfloor Heating Control with External Temperature Compensation. In Proceedings of the 14th International Conference on Informatics in Control, Automation and Robotics, Madrid, Spain, 26–28 July 2017; pp. 629–636. [CrossRef]
18. Curtiss, P.S. Examples of Neural Networks Used for Building System Control and Energy Management. *ASHRAE Trans.* **1997**, *103*, 909.
19. Hasan, A.; Kurnitski, J.; Jokiranta, K. A combined low temperature water heating system consisting of radiators and floor heating. *Energy Build.* **2009**, *41*, 470–479. [CrossRef]
20. Võsa, K.-V.; Ferrantelli, A.; Kurnitski, J. Annual performance analysis of heat emission in radiator and underfloor heating systems in the European reference room. *E3S Web Conf.* **2019**, *111*, 111. [CrossRef]
21. Kukolj, D.D.; Kuzmanović, S.B.; Levi, E. Design of a PID-like compound fuzzy logic controller. *Eng. Appl. Artif. Intell.* **2001**, *14*, 785–803. [CrossRef]

22. Ostermeier, M.; Müller, J. Automated investigation, evaluation and optimisation of simple heating circuits in building automation. *E3S Web Conf.* **2019**, *111*, 111. [CrossRef]
23. Fiducioso, M.; Curi, S.; Schumacher, B.; Gwerder, M.; Krause, A. Safe Contextual Bayesian Optimization for Sustainable Room Temperature PID Control Tuning. In Proceedings of the Twenty-Eighth International Joint Conference on Artificial Intelligence, Macao, 10–16 August 2019. [CrossRef]
24. Nägele, F.; Kasper, T.; Girod, B. Turning up the heat on obsolete thermostats: A simulation-based comparison of intelligent control approaches for residential heating systems. *Renew. Sustain. Energy Rev.* **2017**, *75*, 1254–1268. [CrossRef]
25. Maivel, M.; Ferrantelli, A.; Kurnitski, J. Experimental determination of radiator, underfloor and air heating emission losses due to stratification and operative temperature variations. *Energy Build.* **2018**, *166*, 220–228. [CrossRef]
26. Võsa, K.-V.; Ferrantelli, A.; Kurnitski, J. Experimental study of radiator, underfloor, ceiling and air heater systems heat emission performance in TUT nZEB test facility. *E3S Web Conf.* **2019**, *111*, 111. [CrossRef]
27. Kull, T.M.; Thalfeldt, M.; Kurnitski, J. Estimating time constants for underfloor heating control. *J. Phys. Conf. Ser.* **2019**, *1343*. [CrossRef]
28. IDA ICE 4.8 SP1, Expert Edition. 2019. Available online: https://www.equa.se/en/ida-ice (accessed on 20 April 2020).
29. Kalamees, T.; Kurnitski, J. Estonian test reference year for energy calculations. *Proc. Est. Acad. Sci. Eng.* **2006**, *12*, 40–58.
30. Ljung, L. *System Identification Toolbox: User's Guide*; MathWorks Incorporated: Natick, MA, USA, 1995.
31. Wetter, M. *Generic Optimization Program User Manual Version 3.0.0*; Lawrence Berkeley National Lab. (LBNL): Berkeley, CA, USA, 2009; pp. 1–108. [CrossRef]
32. Åström, K.J.; Hägglund, T. *Advanced PID Control*; ISA-The Instrumentation, Systems, and Automation Society: Research Triangle Park, NC, USA, 2006; Volume 461.
33. Nord Pool. Available online: https://www.nordpoolgroup.com/historical-market-data/ (accessed on 20 April 2020).
34. Clauß, J.; Stinner, S.; Sartori, I.; Georges, L. Predictive rule-based control to activate the energy flexibility of Norwegian residential buildings: Case of an air-source heat pump and direct electric heating. *Appl. Energy* **2019**, *237*, 500–518. [CrossRef]
35. *EN 16798-2, Energy Performance of Buildings—Part 2: Indoor Environmental Input Parameters for Design and Assessment of Energy Performance of Buildings Addressing Indoor Air Quality, Thermal Environment, Lighting and Acoustics*; EPB Center: AN Rotterdam, The Netherlands, 2019.